

Received 28 November 2022, accepted 16 December 2022, date of publication 19 December 2022, date of current version 29 December 2022.

Digital Object Identifier 10.1109/ACCESS.2022.3230838

## RESEARCH ARTICLE

# Spatial Index Modulation With the Combination of Both Antenna Indexes and Two Constellations

PING YU<sup>1</sup> AND FUCHUN HUANG<sup>2</sup>

<sup>1</sup>Guangdong Peizheng College, Guangzhou 510830, China

<sup>2</sup>Guangzhou College of Commerce, Guangzhou 511363, China

Corresponding author: Fuchun Huang (20210132@gcc.edu.cn)

This work was supported in part by the Key Research Project of the Guangdong Peizheng College under Grant pzxjzd10; and in part by the Basic and Applied Basic Research Project, Guangzhou Basic Research Plan, under Grant 202201011680.

**ABSTRACT** In this paper, in order to further exploit the antenna index (AI) domain for increasing the spectral efficiency, we propose a new schematic of enhanced generalized spatial modulation with both three dimension constellation and QAM constellation (EGSM-3DQ) to enhance the active AI combinations with the construction of three dimension (3D) signal constellation. In the EGSM-3DQ, a transmit vector symbol (TVS) consists of two spatial vector symbols (SVS) with the aid of one vector index bit, one SVS of which is obtained by modulating three components of a 3D signal symbol on two or three active transmit antennas (TAs) through the 3D Signal Mapper and AI Vector Modulator, another SVS of which is obtained by modulating one or multiple mapped QAM symbols on one or multiple active TAs through the AI Vector Selector. In addition, by jointing the AIs and multiple constellations such as the 3D and QAM, PAM constellations, grouping EGSM (gEGSM) is proposed to develop the group index combinations to increase extra index information. Finally, the comparisons of squared minimum Euclidean distances (MED) and the average bit error probability are provided. Simulation results show that the proposed schemes improve the bit error rate performance as compared with conventional systems.

**INDEX TERMS** Enhanced generalized spatial modulation (EGSM), three dimension (3D) constellation, grouping EGSM (gEGSM), minimum Euclidean distance.


## I. INTRODUCTION

In the past decade years, index modulation technologies, which transmit one or multiple transmit data symbol by activating one transmit antenna (TA) or multiple TAs in the total of TAs, are wisely researched for improving the spectral efficiency (SE) in wireless communication systems.

### A. RELATED WORK

In spatial modulation (SM) [1] that only activates only one TA to convey data symbol (e.g. quadrature amplitude modulation/phase shift modulation (QAM/PSK)), the spatial index bits depend entirely on the number of TAs, which need to satisfy the power of two, i.e.,  $\log_2 N_t$ , where  $N_t$  is the number of TAs. Although the SM relaxes the problem of both the

inter channel interference and inter antenna synchronization, the number of TAs increases exponentially by the power of two when increasing the spatial index bits. In generalized SM (GSM) [2], [3], [4], in order to relax the number of TAs and improve the spatial index bits, the combinations of multiple antenna indexes (AIs) are investigated to activate simultaneously several TAs for the transmission of different data symbols such as QAM/PSK, i.e.,  $\lfloor \log_2 C_{N_t}^{n_a} \rfloor$ , where  $n_a$  is the number of active TAs and  $\lfloor \cdot \rfloor$  is the floor operation. In order to break through the limitations of the single spatial domain, quadrature spatial modulation (QSM) [5] extends the spatial domain to the in-phase and quadrature spatial dimensions. Thus, QSM can achieve more  $\lfloor \log_2 C_{N_t}^1 \rfloor$  information bits than SM in terms of spatial index bits. To further improve the SE while enhancing the bit error rate (BER) performance, a lot of works on generalization of QSM (GQSM) [6], [7], [8]

The associate editor coordinating the review of this manuscript and approving it for publication was Yiming Huo .

have been developed. Although the GQSM systems can achieve  $2n_a \log_2 C_{N_t}^{n_a}$  of spatial index bits by increasing the active AI combinations, the complexity of detection will be relatively increased with the increasing of active TAs in the in-phase and quadrature dimensions. In other words, the number of spatial index bits are increased at the cost of the detection complexity. Quadrature index modulation with three dimension (3D) constellation (QIM-TDC) [9] is proposed to transmit two components of a 3D symbol by using two active TAs in the in-phase dimension and to transmit the remaining one by using one active TA in the quadrature dimension, respectively. Consequently,  $\left\lfloor \log_2 C_{N_t}^2 \right\rfloor + \log_2 C_{N_t}^1$  number of spatial index bits are achieved. In order to further improve the spatial index bits, with the aid of two states of both  $l$  and  $j$ , spatial modulation with spatial constellation (SM-SC) [10] develops the group index domain according to the  $D$  dimensions of the employed data symbol, thus it has  $\left\lfloor \log_2 C_{N_t}^{n_a} \right\rfloor + D$  to be conveyed. However, for the above systems such as QSM, QIM-TDC and SM-SC, the squared minimum Euclidean distance (MED) is changed to  $\frac{2}{E_{av}}$ , where  $E_{av}$  is the average energy per transmit vector symbol (TVS). From this, it will affect the the reliability of communications. In order to avoid this problem while increasing the spatial index bits, on the joint design of active TA(s) and multiple signal constellations, enhanced SM (ESM) [11], [12] is proposed to either transmit one primary symbol (e.g.  $M$ -ary QAM) by using one active TA or transmit two secondary symbols by using two active TAs. Thus, the spatial index bits carried by ESM is  $\log_2(C_{N_t}^1 + 2C_{N_t}^2)$ . In order to not only further carry more spatial index bits but also keep the characteristic of the squared MED (i.e.,  $\frac{4}{E_{av}}$ ), generalized spatial modulation with multi-index modulation (GSM-MIM) [13] has been developed to exploit multiple index domains with the aid of two distinct signal constellations (e.g., pulse amplitude modulation (PAM) and QAM) and the sign  $j$ . Based on the in-phase and quadrature dimensions, a lot of works [14], [15] on developing more spatial index bits have done and achieved the higher SE. In [14], improved QSM (IQSM) is proposed to activate two out of all TAs in the in-phase and quadrature dimensions for transmitting the real and imaginary parts of two signal symbols, respectively. Thus, the number of spatial index bits transmitted by the IQSM system are increased to  $2 \cdot \left\lfloor \log_2 \frac{N_t!}{2^{l(N_t-2)!}} \right\rfloor$ . In double GSM (DGSM) [15], all AI combinations of activating one or more than one TA are developed to convey the spatial index bits that is  $2 \cdot \left\lfloor \log_2(C_{N_t}^1 + \dots + C_{N_t}^{N_t/2+1}) \right\rfloor$ . In order to make the best use of the resource of the idle TAs in large scale TAs, all TAs are divided into multiple groups [16], [17], [18]. In [16], the spatial index bits carried by grouping GSM (gGSM) is  $G \cdot \left\lfloor \log_2(N_t/G) \right\rfloor$ . However, grouping GSM only exploits the spatial index bits in one spatial domain, so as to limit the exploiting of the spatial index information. From this, the in-phase and quadrature dimensions of the spatial domain are considered. In both GQSM [17] and parallel QSM

(PQSM) [18], each group of which performs the design principle of QSM, the spatial index bits the PQSM and GQSM can convey are  $2G \cdot \log_2 \frac{N_t}{G}$ . However, the GQSM and PQSM schemes do not consider the design of signal constellations. In other words, the spatial gain from signal constellations and the spatial index information exploited by jointing design of both signal constellations and the active TAs need to be further developed.

## B. MOTIVATION AND CONTRIBUTION

Considering previous literatures, inspired by the design idea of GSM-MIM and DGSM, a new design of enhancing the active AI combinations using the 3D constellation, called as enhanced generalized spatial modulation with both 3D constellation and QAM constellation (EGSM-3DQ), is proposed to increase the SE. Then, in order to further exploit the index domain, by jointing the AI combinations and multiple constellations, the grouping EGSM scheme is proposed and develop the group index information. The main contributions of this paper can be summarized as follows:

- In view of the resource of  $N_t$  TAs and the utilization of three components in the 3D signal constellation, the EGSM-3DQ scheme expands the number of the active AI combinations with the 3D constellation. In the EGSM-3DQ, the total of  $N_t$  TAs are divided into two groups of  $TX_1$  and  $TX_2$  TAs. Then, two or three out of the group of  $TX_1$  TAs are used to modulate the 3D constellation point (CP) symbol  $\bar{s}^{3D}(m_x, m_y, m_z)$  for forming a spatial vector symbol (SVS)  $\mathbf{X}$ . The active TA(s) from the group of  $TX_2$  TAs is(are) used to modulate the mapped QAM symbol(s) for forming other one SVS  $\tilde{\mathbf{X}}$ . With the Vector Combiner, using one extra bit to determine the form of TVS from the combinations of  $\mathbf{X}$  and  $\tilde{\mathbf{X}}$ .
- Specifically, in order to be capable of exploiting more spatial index bits by expanding the active AI combinations, two out of  $TX_1$  TAs are activated to respectively modulate two components of the spatial signal point (SSP) that has four forms:  $\{(m_x, m_y + jm_z), (jm_x, m_y + jm_z), (m_y + jm_z, m_x), (m_y + jm_z, jm_x)\}$ , which are obtained by converting a 3D symbol  $\bar{s}^{3D}(m_x, m_y, m_z)$  with the aid of the 3D→2D Converter. Thus, it has  $4C_{TX_1}^2$  AI vectors to be designed to four forms of SSP symbols. On the other hand, three out of  $TX_1$  TAs are activated to respectively modulate three components of the SSP that has two forms:  $\{(m_x, m_y, m_z), (jm_x, jm_y, jm_z)\}$ , which are obtained by one key controller controlling two states of  $\{1, j\}$ . In this case, we can design  $2C_{TX_1}^3$  AI vectors. Consequently, there exist  $4C_{TX_1}^2 + 2C_{TX_1}^3$  AI vectors that are candidate for being constructed into an AI vector set for carrying spatial index bits.
- In order to further exploit the index domain for increasing the SE, with the 3D constellation and the QAM and PAM constellations, grouping EGSM (gEGSM) is

TABLE 1. List of abbreviations.

SM	Spatial Modulation
GSM	Generalized Spatial Modulation
QSM	Quadrature Spatial Modulation
GQSM	Generalization of QSM
QIM-TDC	Quadrature Index Modulation with 3D Constellation
SM-SC	Spatial Modulation with Spatial Constellation
ESM	Enhanced SM
GSM-MIM	GSM with Multi-Index Modulation
DGSM	Double GSM
IQSM	Improved QSM
GQSM	Generalized QSM
PQSM	Parallel QSM
EGSM-3DQ	Enhanced GSM with 3D and QAM constellations
gEGSM	Grouping EGSM
TA	Transmit antenna
SE	Spectral Efficiency
QAM	Quadrature Amplitude Modulation
PSK	Phase Shift Modulation
PAM	Pulse Amplitude Modulation
AI	Antenna Index
BER	Bit Error Rate
SSP	Spatial Signal Point
GI	Group Index
3D	Three Dimension
MED	Minimum Euclidean Distance
TVS	Transmit Vector Symbol
CP	Constellation Point
SVS	Spatial Vector Symbol
$\bar{s}^{3D}$	3D CP Symbol

developed and exploits the group index combinations to increase extra index information.

- We analyze the squared MED between the TVSs, which verify the advantage of the proposed schemes as compared with GSM-MIM. Simulation results are conducted to demonstrated that the proposed schemes outperform other schemes in terms of BER performance.

The rest of the paper is organized as follows. In Section II, we introduce system model of EGSM-3DQ and an improved 3D signal constellation. In Section III, system model of gEGSM is introduced. In Section IV, the squared MED comparison and the average bit error probability are presented. Finally, simulation results are given and discussed in Sections V and our conclusions is given in Section VI.

The abbreviations for various systems used throughout the paper are listed in TABLE 1

## II. PROPOSED EGSM-3DQ

### A. SYSTEM MODEL

Let us consider that the schematic framework of the EGSM-3DQ system with  $N_t$  transmit antennas (TAs) and  $N_r$  receiver antennas, as is shown in Fig. 1. Note that the number of TAs are consist of two groups,  $TX_1$  and  $TX_2$  TAs (i.e., we define  $N_t = TX_1 + TX_2$ ),  $TX_1$  TAs of which for transmitting a 3D constellation point (CP) symbol  $\bar{s}^{3D}$  and  $TX_2$  TAs of which for transmitting  $\tau$  QAM CP symbols:  $s^1, \dots, s^\tau$ , ( $1 \leq \tau < TX_2$ ), respectively. Specifically, assume that a total of  $\mathbf{m} = \log_2 N + I_{SIB} + \tau \cdot \log_2 M$  information bits, which are divided into three blocks: the mapping 3D CP bits ( $\log_2 N$ ) with the  $N$ -ary 3D constellation, the spatial index bits ( $I_{SIB}$ ) and the mapping QAM CP bits ( $\tau \cdot \log_2 M$ )

with the QAM constellation, are entered the transmitter of the proposed EGSM-3DQ in each TVS duration, where  $N$  and  $M$  respectively denote the modulation orders of 3D constellation and QAM constellation,  $\tau$  denotes the number of mapped QAM symbols. Furthermore,  $I_{SIB}$ , denoting the number of spatial index bits, is divided into three groups:  $I_A, I_B$  and  $I_V$ .

For both the group of  $I_A$  and the block of mapping 3D CP bits ( $\log_2 N$ ), the 3D Signal Mapper and AI Vector Modulator encode them into a SVS  $\mathbf{X}_{\bar{D}}$ . The detailed design is as follows: As depicted in Fig. 1, the block of mapping 3D CP bits, containing  $\log_2 N$  bits, is mapped into a 3D CP symbol  $\bar{s}^{3D}(m_x, m_y, m_z)$  from the  $N$ -3D constellation that will be designed in II-B. The group of  $I_A$ , containing  $\log_2(N_A), N_A = 2^{\lfloor \log_2 |\Delta| \rfloor}$  information bits, is converted into a decimal number  $\bar{D}$ , ( $1 \leq \bar{D} \leq N_A$ ) by converting the  $I_A$  into a decimal, where  $\lfloor \cdot \rfloor$  denotes the floor operation. Note that  $|\Delta|$  denotes the number of all AI vectors in the set  $\Delta = \{\Delta_1, \Delta_2\}$  that has  $C_{TX1}^2 \times 4 + C_{TX1}^3 \times 2$  ( $|\Delta_1| = C_{TX1}^2 \times 4, |\Delta_2| = C_{TX1}^3 \times 2$ ) possible AI vectors for activating  $\alpha, \alpha \in \{2, 3\}$  out of  $TX_1$  TAs, and will be introduced in II-C, where  $C_y^x$  denotes combination operation. After entering the group of bits into the Size Comparator, according to judgment of the Size Comparator, there exists two outputs:

- 1) If  $\bar{D} \leq |\Delta_1|$ , the Size Comparator outputs the AI number  $\lambda, \lambda \in \{1, \dots, |\Delta_1|\}$ , which is fed into not only the Two-State Output-I but also the AI Vector Selector-I and the Ceil Algorithm Device. In this case, the parameter  $\kappa_1$  is set to "0" (i.e.,  $\kappa_1 = 0$ ), which is used to switch the  $\kappa_1$  up for feeding the 3D CP symbol  $\bar{s}^{3D}(m_x, m_y, m_z)$  into the 3D→2D Converter. Then, according to the output  $\delta$  ( $1 \leq \delta \leq 4$ ) of the Ceil Algorithm Device whose expression of the algorithm is  $\delta = \text{Ceil}(\lambda / C_{TX1}^2)$ , the 3D→2D Converter convert the 3D symbol  $\bar{s}^{3D}(m_x, m_y, m_z)$  into one SSP symbol  $Q_\delta^2$  from four SSPs  $Q^2 = \{Q_1^2, \dots, Q_4^2\} = \{(m_x, m_y + jm_z), (jm_x, m_y + jm_z), (m_y + jm_z, m_x), (m_y + jm_z, jm_x)\}$ . In the AI Vector Selector-I, the AI number  $\lambda$  is employed to select a specific  $\mathbf{V}_\lambda$ , which containing two non-zero elements equaling to "1", from the AI vector set

$$\Delta_1 = \left\{ \underbrace{\mathbf{V}_1, \dots, \mathbf{V}_{C_{TX1}^2}}_{Q_1^2}, \underbrace{\mathbf{V}_{C_{TX1}^2+1}, \dots, \mathbf{V}_{2C_{TX1}^2}}_{Q_2^2}, \underbrace{\mathbf{V}_{2C_{TX1}^2+1}, \dots, \mathbf{V}_{3C_{TX1}^2}}_{Q_3^2}, \underbrace{\mathbf{V}_{3C_{TX1}^2+1}, \dots, \mathbf{V}_{|\Delta_1|}}_{Q_4^2} \right\}$$

Note that, from the design of the set  $\Delta_1, \mathbf{V}_{(\delta-1) \cdot C_{TX1}^2+1}, \dots, \mathbf{V}_{\delta \cdot C_{TX1}^2}$  are used to modulate the corresponding SSP symbol  $Q_\delta^2$ . According to the selected AI vector  $\mathbf{V}_\lambda$ , two components of the corresponding SSP symbol  $Q_\delta^2$  are modulated on two out of  $TX_1$  TAs activated by the AI vector  $\mathbf{V}_\lambda$ , resulting in a SVS  $\mathbf{X}_\lambda$ .

- 2) If  $\bar{D} > |\Delta_1|$ , the Size Comparator outputs the AI number  $\beta, \beta \in \{1, \dots, |\Delta_2|\}$ , which is fed into not

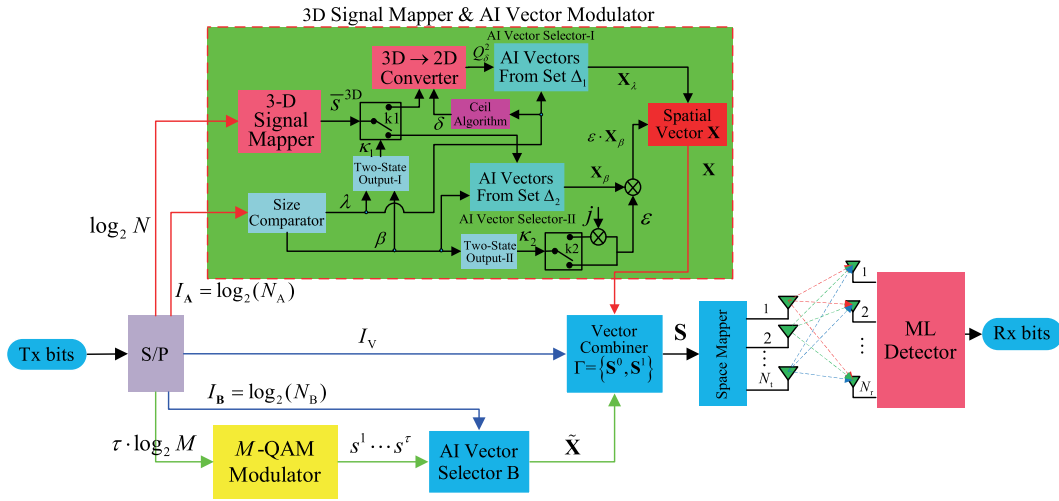


FIGURE 1. Transceiver of EGSM-3DQ.

only these two Two-State Output-I, II but also the AI Vector Selector-II. In this case, the parameter  $\kappa_1$  is set to “1” (i.e.,  $\kappa_1 = 1$ ) in the Two-State-Output-I, which is used to switch the  $k_1$  down for feeding directly the 3D CP symbol  $\bar{s}^{3D}(m_x, m_y, m_z)$  into the AI Vector Selector-II. Then, according to the AI number  $\beta$ , a specific  $\mathbf{V}'_\beta$ , which containing three non-zero elements equaling to “1”, is selected from the AI vector set  $\Delta_2 = \{\mathbf{V}'_1, \mathbf{V}'_2, \dots, \mathbf{V}'_{|\Delta_2|}\}$ , and used to activate three out of  $TX_1$  TAs for respectively modulating three components of the  $\bar{s}^{3D}(m_x, m_y, m_z)$ , resulting in a SVS  $\mathbf{X}$ . Due to producing the same SVS  $\mathbf{X}$ , this will cause unrecoverable detection errors at the receiver. In order to avoid this problem. With the aid of the Two-State Output-II, if  $\beta \leq C_{N_t}^3$ ,  $\kappa_2$  is set to “0” (i.e.,  $\kappa_2 = 0$ ), and is used to switch the key  $k_2$  down. Thus  $\varepsilon = 1$ . Otherwise,  $\varepsilon = j$ . Consequently, according to the key  $k_2$  control, the expression of  $\varepsilon \cdot \mathbf{X}_\beta$  may be given by

$$\varepsilon \cdot \mathbf{X}_\beta = \begin{cases} \mathbf{X}_\beta, & \kappa_2 = 0 \\ j\mathbf{X}_\beta, & \kappa_2 = 1 \end{cases}$$

Finally, we can obtain the SVS  $\mathbf{X}_{\bar{D}}$  for  $TX_1$  TAs, as follows

$$\mathbf{X} = \mathbf{X}_{\bar{D}} = \begin{cases} \mathbf{X}_\lambda, & \bar{D} \leq |\Delta_1| \\ \varepsilon \cdot \mathbf{X}_\beta = \begin{cases} \mathbf{X}_\beta, & \kappa_2 = 0 \\ j\mathbf{X}_\beta, & \kappa_2 = 1 \end{cases}, & \bar{D} > |\Delta_1|. \end{cases} \quad (1)$$

Note that,

$$\bar{D} = \begin{cases} \lambda, & \bar{D} \leq |\Delta_1| \\ |\Delta_1| + \beta, & \bar{D} > |\Delta_1|. \end{cases}$$

Furthermore, for the second group of  $I_B$ , containing  $\log_2(N_B)$ ,  $N_B = 2^{\lceil \log_2(C_{TX_2}^r) \rceil}$  information bits, it is used to select a specific AI vector  $\bar{\mathbf{V}}_\xi$ ,  $\xi \in \{1, \dots, N_B\}$  from the AI

vector set  $\Lambda = \{\bar{\mathbf{V}}_1, \bar{\mathbf{V}}_2, \dots, \bar{\mathbf{V}}_{N_B}\}$  to modulate  $\tau$   $M$ -QAM ( $M \geq 2$ ) symbol(s) (e.g.  $s^1, \dots, s^\tau$ ) obtained by mapping the  $\tau \cdot \log_2 M$  information bits, resulting in a spatial vector symbol  $\tilde{\mathbf{X}}$ , where  $\Lambda \in \Omega$ ,  $\Omega$  denotes the set that contains all possible AI vectors that can activate  $\tau$  out of  $TX_2$  TAs. Note that, each vector in the set  $\Lambda$  has  $\tau$  non-elements equaling to “1” to activate  $\tau$  TAs, and when  $M = 2$ , the 2-QAM constellation:  $\{2 + 2j, -2 - 2j\}$  is employed.

To further achieve one more information bit, we utilize two vector symbols  $\mathbf{X}, \tilde{\mathbf{X}}$  to construct two different forms of TVS, i.e.,  $\{\mathbf{S}^0, \mathbf{S}^1\}$ , one of which is determined by one bit. These two different TVS forms may be designed as follows

$$\mathbf{S} = \begin{cases} \mathbf{S}^0 = [\mathbf{X} \tilde{\mathbf{X}}]^T, & I_V = 0 \\ \mathbf{S}^1 = [\tilde{\mathbf{X}} \mathbf{X}]^T, & I_V = 1 \end{cases} \quad (2)$$

where  $I_V$  is one information bit that is used to select one of the two different forms of TVSs to be transmitted. Specifically, in the Vector Combiner of Fig. 1, the last group of  $I_V$ , only containing one information bit, is fed into the Vector Combiner and then select a TVS from  $\{\mathbf{S}^0, \mathbf{S}^1\}$ . Finally, through the Space Mapper, the selected TVS  $\mathbf{S}$  is mapped on  $N_t$  TAs.

To further illustrate the working principle of the proposed EGSM-3DQ, examples of forming a EGSM-3DQ symbol are given in TABLE 2. Assumed that  $N_t = 8$ ,  $TX_1 = TX_2 = 4$ ,  $I_{SIB} = \underbrace{b_0, b_1, b_2, b_3, b_4}_{I_A}, \underbrace{b_5, b_6}_{I_B}, \underbrace{b_7}_{I_V}$  bits, the mapped 3D

and QAM symbols are  $\bar{s}^{3D} = (m_x, m_y, m_z)$  and one  $s^1$ , respectively. Moreover, the AI vector set  $\Delta$  is provided by the example of (9). In Table 2, the AI vector  $\bar{\mathbf{V}}_{\bar{D}}$  with the AI number  $\bar{D}$  is obtained by the information bits  $\{b_0, b_1, b_2, b_3, b_4\}$ , where  $\mathbf{P}_1 = [0 \ 0 \ m_x \ m_y + jm_z \ s^1 \ 0 \ 0 \ 0]^T$ ,  $\mathbf{P}_2 = [0 \ m_y + jm_z \ 0 \ m_x \ 0 \ s^1 \ 0 \ 0]^T$ ,  $\mathbf{P}_3 = [0 \ 0 \ s^1 \ 0 \ 0 \ m_y + jm_z \ jm_x \ 0]^T$ ,  $\mathbf{P}_4 = [0 \ 0 \ 0 \ s^1 \ jm_x \ jm_y \ 0 \ jm_z]^T$ .

**TABLE 2.** Examples of forming a TVS with  $N_t = 8, TX_1 = TX_2 = 4, I_{SIB} = 8$  bits.

	$\overbrace{b_0, b_1, b_2, b_3, b_4, b_5, b_6, b_7}^{I_A, I_B, I_C, I_D}$			
	00101 00 0	01010 01 0	10101 10 1	11101 11 1
$D$	6	11	22	30
$\xi$	1	2	3	4
$I_V$	1	1	2	2
$V_\lambda$ or $V'_\beta$	$[0\ 0\ a\ b + jc]^T$	$[0\ b + jc\ 0\ a]^T$	$[0\ b + jc\ ja\ 0]^T$	$[ja\ jb\ 0\ jc]^T$
$V_\xi$	$[1\ 0\ 0\ 0]^T$	$[0\ 1\ 0\ 0]^T$	$[0\ 0\ 1\ 0]^T$	$[0\ 0\ 0\ 1]^T$
$S$	$P_1$	$P_2$	$P_3$	$P_4$

**TABLE 3.** Examples of 8, 16, 32, 64-ary 3D constellations.

Modulation order	3D constellation points
8-ary	$(\pm 2, \pm 2, \pm 2)$
16-ary	$\{(\pm 2, \pm 2, \pm 2), (\pm 4, \pm 2, \pm 2)\}$
32-ary	$\left\{ \begin{array}{l} (\pm 2, \pm 2, \pm 2), (\pm 4, \pm 2, \pm 2), \\ (\pm 2, \pm 4, \pm 2), (\pm 2, \pm 2, \pm 4) \end{array} \right\}$
64-ary	$\left\{ \begin{array}{l} (\pm 2, \pm 2, \pm 2), (\pm 4, \pm 2, \pm 2), \\ (\pm 2, \pm 4, \pm 2), (\pm 2, \pm 2, \pm 4), \\ (\pm 4, \pm 4, \pm 2), (\pm 4, \pm 2, \pm 4), \\ (\pm 2, \pm 4, \pm 4), (\pm 2, \pm 2, \pm 6) \end{array} \right\}$

Based on the above design, the SE (bits/s/Hz) of the EGSM-3DQ can be calculated by

$$\eta = \log_2 N + \left[ \log_2(4C_{TX1}^2 + 2C_{TX1}^2) \right] + \tau \cdot \log_2 M + \left[ \log_2(C_{TX2}^T) \right] + 1 \quad (3)$$

**B. 3D CONSTELLATION FOR EGSM-3DQ**

In view of theoretical analysis of the squared MED  $\bar{d}_{S, \min}^2 = \frac{4}{E_{av}^{GSM-MIM}}$  in the GSM-MIM system, where  $E_{av}^{GSM-MIM}$  denotes the average energy of each TVS, three components of the 3D constellation are taken from the values:  $\{\pm 2, \pm 4, \dots, \pm 2Z\}$ . Thus, the design of the 3D constellation can be as follows:

$$\bar{s}^{3D} = (m_x, m_y, m_z), m_x, m_y, m_z \in \{\pm 2, \pm 4, \pm 2Z\} \quad (4)$$

where  $Z$  denotes the integer operation. For example, Table 3 provides 8, 16, 32, 64-ary 3D constellations.

**C. DESIGN OF SPATIAL VECTOR SYMBOL FOR  $TX_1$  TAs**

Through exploiting the spatial domain from the resource of  $TX_1$  TAs, the expansion of the number of AI vectors is to aim at increasing the SE by carrying more extra index information bits. According to the characteristics of dimensions of a mapped 3D CP symbol in the 3D constellation, all AI vectors, which can activate two or three TAs, can be designed to directly transmit a 3D CP symbol. The design methodology of the AI vectors is as follows:

- 1) When two out of  $TX_1$  TAs are activated, one of the two active TAs is used to modulate the component  $m_x$  of the mapped 3D symbol  $\bar{s}^{3D}(m_x, m_y, m_z)$ . The other one is used to modulate the remaining two components  $m_y, m_z$  of the mapped 3D symbol. Thus, in order to perform that the mapped 3D symbol  $\bar{s}^{3D}(m_x, m_y, m_z)$  are directly transmitted by two active TAs, the 3D  $\rightarrow$

2D Converter is employed to convert the 3D symbol  $\bar{s}^{3D}(m_x, m_y, m_z)$  into the following SSP forms:

$$\begin{aligned} \bar{s}^{3D} &= (m_x, m_y, m_z) \\ &\Rightarrow \left\{ \begin{array}{l} (m_x, m_y + jm_z), (jm_x, m_y + jm_z) \\ (m_y + jm_z, m_x), (m_y + jm_z, jm_x) \end{array} \right\} \quad (5) \end{aligned}$$

In this case, we can design  $4C_{TX1}^2$  AI vectors, which are given by (6), as shown at the bottom of the next page, where the  $a, b, c$  positions are replaced by  $m_x, m_y, m_z$  values of a 3D CP symbol, respectively.

- 2) When three out of  $TX_1$  TAs are activated, each active TA is used to modulate each component  $m_\chi, \chi \in \{x, y, z\}$  of the mapped 3D symbol  $\bar{s}^{3D}(m_x, m_y, m_z)$ , respectively. Furthermore, with the aid of the k2 controller controlling two states of  $\{1, j\}$  in Fig. 1, the mapped 3D symbol  $\bar{s}^{3D}(m_x, m_y, m_z)$  may be converted into the following symbol forms:

$$\begin{aligned} \bar{s}^{3D} &= (m_x, m_y, m_z) \\ &\Rightarrow \left\{ \tilde{s}_1^{3D}(m_x, m_y, m_z), \tilde{s}_2^{3D}(jm_x, jm_y, jm_z) \right\}. \quad (7) \end{aligned}$$

Thus, we can design  $2C_{N_t}^3$  AI vectors for transmitting the three components of the mapped 3D symbol  $\bar{s}^{3D}(m_x, m_y, m_z)$ , which are given by

$$\Delta_2 = \begin{bmatrix} a & a & \dots & 0 & ja & ja & \dots & 0 \\ b & b & \vdots & 0 & jb & jb & \vdots & 0 \\ c & 0 & \dots & \vdots & jc & 0 & \dots & \vdots \\ 0 & c & \vdots & a & 0 & jc & \vdots & ja \\ \vdots & \vdots & 0 & b & \vdots & \vdots & 0 & jb \\ 0 & 0 & \dots & c & 0 & 0 & \dots & jc \end{bmatrix} \quad (8)$$

$\underbrace{\hspace{10em}}_{C_{TX1}^3 \text{ AI vectors}} \quad \underbrace{\hspace{10em}}_{C_{TX1}^3 \text{ AI vectors}}$

where the  $a, b, c$  positions are replaced by the three components  $m_x, m_y, m_z$  of a 3D CP symbol, respectively.

Consequently, based on the above mentioned design, we can construct a set  $\Delta = \{\Delta_1, \Delta_2\}$  with  $C_{TX1}^2 \times 4 + C_{TX1}^3 \times 2$  AI vectors. For instance, assumed that  $TX_1 = 4$ , an AI vector set that has a total of  $C_4^2 \times 4 + C_4^3 \times 2 = 32$  AI vectors is given by (9), as shown at the bottom of the next page. It can be obtained from (9), five extra index information bits can be achieved.

**III. PROPOSED GROUPING EGSM SCHEME**

In this section, on the basis of the design structure of the EGSM-3DQ, we propose the gEGSM scheme, in which not only the spatial index domain is further exploited to increase the SE but also the squared MED is further increased for enhancing the reliability of wireless communications.

The system model for the gEGSM equipped with  $N_t = TX_1 + TX_2 + TX_3$  TAs is depicted in Fig. 2, where the Vector

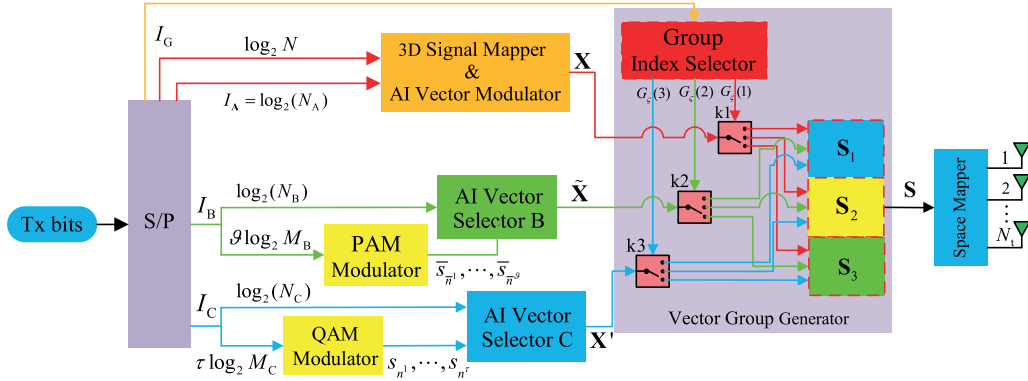


FIGURE 2. System model of gEGSM.

Group Generator is designed for exploiting the extra information  $I_G$ . In the Vector Group Generator, the resulted SVSs:  $\mathbf{X}, \tilde{\mathbf{X}}, \mathbf{X}'$  are fed into the three vector blocks (e.g.  $\mathbf{S}_1, \mathbf{S}_2, \mathbf{S}_3$ ) through the controlling of three Switches with the information bits  $I_G$ . Specifically, as shown in the left of Fig. 2, the TX bits  $\mathbf{m}$  are divided into five data sub-streams:  $\log_2 N$ ,  $I_A$ ,  $I_G$ ,  $I_B$  and  $I_C$ . Furthermore, according to the design of the 3D Signal Mapper and AI Vector Modulator in the EGSM-3DQ scheme, the two sub-streams of both  $\log_2 N$  and  $I_A$  containing  $\log_2 N_A$  bits are modulated into a SVS

$\mathbf{X}$  to be transmitted on  $TX1$  TAs. For the sub-stream of  $I_B$ , which are further divided into  $\log_2 N_B$  and  $\vartheta \log_2 M_B$  bits,  $\vartheta \log_2 M_B$  bits by the PAM Modulator are modulated into  $\vartheta M_B$ -PAM symbols:  $\bar{s}_{\bar{n}^1}, \dots, \bar{s}_{\bar{n}^\vartheta}$  from the constellation set  $\Gamma = \{\pm 2, \dots, \pm 2\mu', \pm 2j, \dots, \pm 2\bar{\mu}'j\}$ ,  $\mu', \bar{\mu}' \in \tilde{N}$ ,  $\tilde{N}$  denotes the natural number. Then,  $\log_2 N_B, N_B = 2^{\lceil \log_2(C_{TX2}^\vartheta) \rceil}$  bits by the AI Vector Selector B are used to select a specific AI vector  $\mathbf{B}_x, x \in \{1, \dots, N_B\}$  from the AI vector set  $\mathbf{B} = \{\mathbf{B}_1, \mathbf{B}_2, \dots, \mathbf{B}_{N_B}\}$  to modulate  $\vartheta$  PAM symbols, resulting in a SVS  $\tilde{\mathbf{X}}$ , where  $\mathbf{B} \in \bar{\Omega}$ ,  $\bar{\Omega}$  denotes the

$$\Delta_1 = \begin{bmatrix} a & a & 0 & 0 & b+jc & b+jc & 0 & 0 & ja & ja & 0 & 0 & b+jc & b+jc & 0 & 0 \\ b+jc & 0 & \vdots & 0 & a & 0 & \vdots & 0 & b+jc & 0 & \vdots & 0 & aj & 0 & \vdots & 0 \\ \vdots & b+jc & \cdots & \vdots & \vdots & a & \cdots & \vdots & \vdots & b+jc & \cdots & \vdots & \vdots & aj & \cdots & \vdots \\ \vdots & \vdots & \vdots & \vdots & \vdots & \vdots & 0 & \vdots & \vdots & \vdots & \vdots & \vdots & \vdots & \vdots & \vdots & \vdots \\ 0 & 0 & 0 & a & 0 & 0 & \vdots & b+jc & 0 & 0 & 0 & ja & 0 & 0 & 0 & b+jc \\ 0 & 0 & 0 & b+jc & 0 & 0 & 0 & a & 0 & 0 & 0 & b+jc & 0 & 0 & 0 & aj \end{bmatrix} \quad (6)$$

$\underbrace{\hspace{15em}}_{C_{TX1}^2 \text{ AI vectors}} \quad \underbrace{\hspace{15em}}_{C_{TX1}^2 \text{ AI vectors}} \quad \underbrace{\hspace{15em}}_{C_{TX1}^2 \text{ AI vectors}} \quad \underbrace{\hspace{15em}}_{C_{TX1}^2 \text{ AI vectors}}$

$$\Delta = \begin{bmatrix} a & a & a & 0 & 0 & 0 & b+jc & b+jc & b+jc & 0 & 0 & 0 \\ b+jc & 0 & 0 & a & a & 0 & a & 0 & 0 & b+jc & b+jc & 0 \\ 0 & b+jc & 0 & b+jc & 0 & a & 0 & a & 0 & a & 0 & b+jc \\ 0 & 0 & b+jc & 0 & b+jc & b+jc & 0 & 0 & a & 0 & a & a \end{bmatrix} \quad (9)$$

$\underbrace{\hspace{15em}}_{C_4^2 \text{ AI vectors}} \quad \underbrace{\hspace{15em}}_{C_4^2 \text{ AI vectors}} \quad \underbrace{\hspace{15em}}_{C_4^1 \text{ AI vectors}} \quad \underbrace{\hspace{15em}}_{C_4^1 \text{ AI vectors}}$

set that contains all possible AI vectors that can activate  $\vartheta$  out of  $TX_2$  TAs. Similarly, the sub-stream of  $I_C$  are further divided into  $\log_2 N_C$  and  $\tau \log_2 M_C$  bits.  $\tau \log_2 M_C$  bits by the QAM Modulator are modulated into  $\tau M_C$ -QAM symbols:  $s_{n^1}, \dots, s_{n^\tau}$ . Then, in the AI Vector Selector  $C$ ,  $s_{n^1}, \dots, s_{n^\tau}$  symbols are modulated by the specific AI vector  $C_y, y \in \{1, \dots, N_C\}$  with the  $\log_2 N_C, N_C = 2^{\lceil \log_2(C_{TX3}^\tau) \rceil}$  bits on  $\tau$  active TAs of  $TX_3$  TAs, resulting in a SVS  $X'$ , where  $C_y$  is from the AI vector set  $C = \{\bar{C}_1, \bar{C}_2, \dots, \bar{C}_{N_C}\}$  and  $C \in \Omega'$ ,  $\Omega'$  denotes the set that contains all possible AI vectors that can activate  $\tau$  out of  $TX_3$  TAs.

Furthermore, in order to exploit more extra index bits, the Vector Group Generator is designed. Specifically, with the aid of the Group Index Selector, the Vector Group Generator feeds the three SVSs  $X, \tilde{X}, X'$  into the corresponding vector blocks (e.g.  $S_1, S_2, S_3$ ). Since the three SVSs  $X, \tilde{X}, X'$  are different, according to the permutation of them, they can be formed into different group index patterns for achieving extra index bits. Hence, in the Group Index Selector, the set of group index patterns can be designed as

$$G = \{G_1, G_2, G_3, G_4, G_5, G_6\} = \{[1, 2, 3], [1, 3, 2], [2, 1, 3], [2, 3, 1], [3, 1, 2], [3, 2, 1]\}, \quad (10)$$

where three components  $[G_\zeta(1), G_\zeta(2), G_\zeta(3)]$  of the specific pattern  $G_\zeta$  with the group index  $\zeta$  that is the decimal representation of  $I_G$  bits, are used to control three Switches: k1, k2, k3 for feeding three SVSs into the specific vector blocks (e.g.  $S_1, S_2, S_3$ ), respectively. For the sake of transmitting the integer multiple of one bit, only four group index patterns of  $G$  are considered as legitimate, the remaining is not considered. Without loss of generality, the group index set may be designed as  $G = \{G_1, G_2, G_3, G_4\}$ . To further illustrate the design principle of the Group Index Selector, an example is provided. Assumed that  $I_G = [1 0]$ , it has  $\zeta = 3$ , and then  $G_3 = [G_3(1), G_3(2), G_3(3)] = [2, 1, 3]$  is selected. In this case, since  $G_3(1) = 2$ , the SVS  $X$  is fed into the 2-nd vector block  $S_2$  through the control of Switch k1. Similarly, since  $G_3(2) = 1$  and  $G_3(3) = 3$ , the two SVS  $\tilde{X}, X'$ , under the control of two switches of both k2 and k3, are fed into the 1-st and 3-rd vector blocks  $S_2, S_3$ , respectively. Finally, a TVS symbol is obtained as  $S = [\tilde{X}, X, X']^T$ .

Based on the above mentioned design and analysis, the SE of gEGSM can be expressed as

$$\eta = \log_2 N + \left[ \log_2(4C_{TX1}^2 + 2C_{TX1}^3) \right] + \vartheta \cdot \log_2 M_B + \left[ \log_2 C_{TX2}^\vartheta \right] + \tau \cdot \log_2 M_C + \left[ \log_2 C_{TX3}^\tau \right] + \left[ \log_2 G \right]. \quad (11)$$

#### IV. ML DETECTION AND PERFORMANCE ANALYSIS

In this section, the maximum-likelihood (ML) detection, the average bit error probability (BEP) and the squared MED comparison are introduced.

#### A. ML DETECTION

At the receiver, the received signal vector of the proposed schemes may be given by

$$y = H \cdot \frac{S}{\sqrt{E_{av}}} + n, \quad (12)$$

where  $y \in C^{N_r \times 1}$ ,  $H \in C^{N_r \times N_t}$  denotes the Rayleigh fading MIMO channel matrix, whose expression can be given by

$$H = \begin{bmatrix} h_{1,1} & h_{1,2} & \dots & h_{1,N_t} \\ h_{2,1} & h_{2,2} & \dots & h_{2,N_t} \\ \vdots & \vdots & \vdots & \vdots \\ h_{N_r,1} & h_{N_r,2} & \dots & h_{N_r,N_t} \end{bmatrix}, \quad (13)$$

each entry  $h_{n_r, \mu}$  of which is an independent and identically distributed (i.i.d) complex Gaussian random variable with  $CN(0, 1)$ , where  $h_{n_r, \mu}, 1 \leq n_r \leq N_r, 1 \leq \mu \leq N_t$  denotes the  $n_r$ -th row and  $\mu$ -th column channel coefficient of the channel matrix  $H$ .  $n \in C^{N_r \times 1}$  is the complex additive white Gaussian noise (AWGN) vector with  $CN(0, \sigma^2 I_{N_r})$ .

Assuming the channel state information is perfectly known, for the better detection of the original information bits, the ML detection is employed for the proposed schemes. For the EGSM-3DQ, the spatial index bits that include the AI bits (e.g.  $I_A, I_B$  and  $I_v$ ) and the symbol index bits ( $\log_2 N$  and  $\tau \cdot \log_2 M$ ) are jointly detected and the detective algorithm may be expressed as

$$\left[ \hat{I}_v, \hat{D}, \hat{N}, \hat{\xi}, \hat{\ell}^1, \dots, \hat{\ell}^\tau \right] = \arg \min_{I_v, \bar{D}, N, \xi, \ell^1, \dots, \ell^\tau} \left\| y - H \cdot \frac{S}{\sqrt{E_{av}}} \right\|^2 \quad (14)$$

where  $\|\cdot\|^2$  denotes the Frobenius norm,  $\hat{I}_v$  denotes the detected vector combining bits.  $\hat{D}, \hat{\xi}$  denote the detected AI vector index.  $\hat{N}, \hat{M}^1, \dots, \hat{M}^\tau$  denotes the modulation order of the detected symbols.

Furthermore, for the gEGSM, the detective algorithm may be expressed as

$$\left[ \hat{\zeta}, \hat{D}, \hat{N}, x, \bar{n}^1, \dots, \bar{n}^\vartheta, y, n^1, \dots, n^\tau \right] = \arg \min_{\zeta, \bar{D}, N, x, \bar{n}^1, \dots, \bar{n}^\vartheta, y, n^1, \dots, n^\tau} \left\| y - H \cdot \frac{S}{\sqrt{E_{av}}} \right\|^2 \quad (15)$$

#### B. AVERAGE BEP ANALYSIS

With the assumption that channel state information is perfectly known. Based on the union bound technique [16], the average BEP of the proposed schemes are calculated out. According to (14) and (15), the average BEP of EGSM-3DQ and gEGSM can be respectively given by (16) and (17), as shown at the bottom of the next page, where  $e(S \rightarrow \hat{S})$  is the total number of erroneous bits for the case of  $S \neq \hat{S}$ ,  $\bar{P}(S \rightarrow \hat{S})$  denotes the average pairwise error probability (PEP). Through taking the expectation of PEP on the channel matrix  $H$  using a moment generating function (MGF)

**TABLE 4.**  $\bar{d}_{S,\min}^2$  comparison between the proposed schemes and GSM-MIM at various SEs.

Schemes	Spectral efficiencies (bits/s/Hz)			
	13	14	15	16
EGSM-3DQ (4, 4)	(1,1,8-3D,4) 4/14	(1,1,8-3D,8) 4/18	(1,2,8-3D,4) 4/16	(1,2,8-3D,4-8) 4/20
GSM-MIM (4, 4)	(3,1,2,16) 4/22	(3,1,2-4,16) 4/28	(3,2,2,8) 4/24	(3,2,2,8-16) 4/28
GSM-MIM (4, 4)	(1,2,2,8) 4/16	(1,2,2,8-16) 4/20	(1,3,2,4-8) 4/18	(1,3,2,8) 4/22

Schemes	Spectral efficiencies (bits/s/Hz)			
	15	16	17	18
EGSM-3DQ (7, 4)	(1,1,8-3D,4) 4/14	(1,1,8-3D,8) 4/18	(1,1,8-3D,16) 4/22	(1,1,16-3D,16) 4/28
EGSM-3DQ (4, 7)	(1,2,8-3D,2) 4/16	(1,2,8-3D,2-4) 4/16	(1,2,8-3D,4) 4/16	(1,2,8-3D,4-8) 4/20
GSM-MIM (7, 4)	(3,1,2,8) 4/18	(3,1,2,16) 4/22	(3,1,2,32) 4/32	(3,1,2,64) 4/54
GSM-MIM (4, 7)	(1,2,2,8) 4/16	(1,2,2,8-16) 4/20	(3,2,2,8) 4/24	(3,2,2,8-16) 4/28
gEGSM (4,2,4)	-	-	A1 4/18	A2 4/22
EGSM-3DQ (4,6)	-	-	(1,2,8-3D,4-8) 4/20	(1,2,8-3D,8) 4/24

from [16], the average PEP can be calculated by (18), as shown at the bottom of the next page, where  $Q(\cdot)$  denotes the Gaussian  $Q$  function,  $h_{n_r,\mu}$  denotes the  $n_r$ -th row and  $\mu$ -th column channel coefficient of the channel matrix  $\mathbf{H}$ ,  $\bar{d}_{S,\min}^2$  denotes the normalized squared MED between the TVSSs.  $\mathbf{S}(\mu)$  and  $\hat{\mathbf{S}}(\mu)$  are the  $\mu$ -th row values of the TVS  $\mathbf{S}$  and detected  $\hat{\mathbf{S}}$ , respectively.

**C. MINIMUM EUCLIDEAN DISTANCE COMPARISON**

According to the (16) and (18), as is known, the bigger the squared MED  $\bar{d}_{S,\min}^2$  is, the smaller the value of the average BEP is. Moreover, in the high signal noise ratio (SNR) region, the asymptotic performance is mainly determined by the squared MED. Hence, in order to outstanding the advantage of the proposed schemes in terms of the squared MEDs, the squared MEDs of the proposed schemes is analyzed in the subsection. After tedious but straightforward calculations for the squared MED of the proposed schemes, the normalized squared MED between the TVSSs can be expressed as

$$\bar{d}_{S,\min}^2 = \min_{\mathbf{S} \neq \hat{\mathbf{S}}} \frac{\|\mathbf{S} - \hat{\mathbf{S}}\|^2}{E_{av}} = \frac{4}{E_{av}} \quad (19)$$

where  $E_{av}$  denotes the average energy of each TVS.

According to (19) and the formulas of the squared MED for other schemes, all normalized squared MEDs between the TVSSs at the same SEs are provided in TABLE 4, where A1=(8-3D,1,4QAM,1,4PAM) and A2=(8-3D,1,8QAM,1,4PAM). For simplicity, we define the

EGSM-3DQ scheme with  $(\alpha, \tau, N, M)$  and GSM-MIM with  $(\tilde{\alpha}, \tilde{\tau}, \tilde{N}, \tilde{M})$  for  $(TX_1, TX_2) = \{(4, 4)^{N_t=8}, (4, 6)^{N_t=10}, (4, 7)^{N_t=11}\}$ , and the gEGSM with  $(N, \vartheta, M_B, \tau, M_C)$  for  $(TX_1, TX_2, TX_3) = \{(4, 2, 4)^{N_t=10}\}$ . Note that  $a$ - $b$  denotes  $a$ -QAM and  $b$ -QAM, which are simultaneously employed in these schemes. From the Table 4, the advantage of the proposed schemes in terms of the squared MED is verified and are bigger than that of GSM-MIM, which is provided in Table 4.

**V. SIMULATION RESULTS AND DISCUSSIONS**

In this section, Simulation results using Monte Carlo method are presented and discussed for the BER performances of the proposed schemes, which are also compared with other IM schemes (e.g. GSM and GSM-MIM) at the same SEs. To make a fair comparison, all IM systems are equipped with the same number of TAs  $N_t$  and receiver antennas  $N_r$ , and detected by the ML detector to retrieve the original information bits. Moreover, the TVSSs are transmitted over the Rayleigh fading MIMO channels, whose channel state information is perfectly known at the receiver. Note that, in our simulation results, we define the EGSM-3DQ scheme with  $(\alpha, \tau, N, M)$  and GSM-MIM with  $(\tilde{\alpha}, \tilde{\tau}, \tilde{N}, \tilde{M})$  for  $(TX_1, TX_2) = \{(4, 4)^{N_t=8}, (4, 6)^{N_t=10}, (4, 7)^{N_t=11}\}$ , and the gEGSM with  $(N, \tau, M_C, \vartheta, M_B)$  for  $(TX_1, TX_2, TX_3) = \{(4, 2, 4)^{N_t=10}\}$ ,  $a$ - $b$  denotes  $a$ -QAM and  $b$ -QAM that are simultaneously employed in these schemes.

In Fig. 3 and Fig. 4, simulation results is provided for the EGSM-3DQ scheme at the SE of 13, 14 bits/s/Hz and  $(N_t, N_r) = (8, 8)$ , and made comparisons with the theoretical results. It can be observed that the simulation results match well with the theoretical results in the high SNR region for the effectiveness of the EGSM-3DQ scheme. Meanwhile, the simulation results for the EGSM-3DQ scheme with (1, 1, 8-3D, 4) and (1, 1, 8-3D, 8) are compared with that of other systems such as GSM-MIM with (1,2,2,8) and (1, 2, 2, 8-16), GSM with  $(n_a = 3, 4-8QAM)$  and  $(n_a = 3, 8QAM)$ , and VBLAST with  $(N_t = 3, 16-32QAM)$  and  $(N_t = 3, 16-32QAM)$ , respectively. It can be observed that the EGSM-3DQ scheme outperforms other systems in terms of BER performance at the SEs of 13, 14 bits/s/Hz.

In Fig. 5, we show the comparisons of the BER performance of the EGSM-3DQ scheme with that of the GSM-MIM system at the SE of 15, 16 bits/s/Hz and  $(N_t, N_r) = (8, 8)$ . According to the analysis of Table 4, the squared MEDs are 4/16 and 4/20 for the EGSM-3DQ with (1, 1, 8-3D, 4) and (1, 1, 8-3D,4-8), and 4/18 and 4/24 for the GSM-MIM

$$P_b \leq \frac{1}{\mathbf{m} \cdot 2^{\mathbf{m}}} \times \sum_{I_v} \sum_{\hat{I}_v} \sum_{\bar{D}} \sum_{\hat{\bar{D}}} \sum_N \sum_{\hat{N}} \sum_{\xi} \sum_{\hat{\xi}} \sum_{M^1} \sum_{\hat{M}^1} \dots \sum_{M^\tau} \sum_{\hat{M}^\tau} \bar{P}(\mathbf{S} \rightarrow \hat{\mathbf{S}}) \cdot e(\mathbf{S} \rightarrow \hat{\mathbf{S}}) \quad (16)$$

$$P_b \leq \frac{1}{\mathbf{m} \cdot 2^{\mathbf{m}}} \times \sum_{\mathcal{S}} \sum_{\hat{\mathcal{S}}} \sum_{\bar{D}} \sum_{\hat{\bar{D}}} \sum_N \sum_{\hat{N}} \sum_x \sum_{\hat{x}} \sum_{M_B^1} \sum_{\hat{M}_B^1} \dots \sum_{M_B^\theta} \sum_{\hat{M}_B^\theta} \sum_y \sum_{\hat{y}} \sum_{M_C^1} \sum_{\hat{M}_C^1} \dots \sum_{M_C^\tau} \sum_{\hat{M}_C^\tau} \bar{P}(\mathbf{S} \rightarrow \hat{\mathbf{S}}) \cdot e(\mathbf{S} \rightarrow \hat{\mathbf{S}}) \quad (17)$$



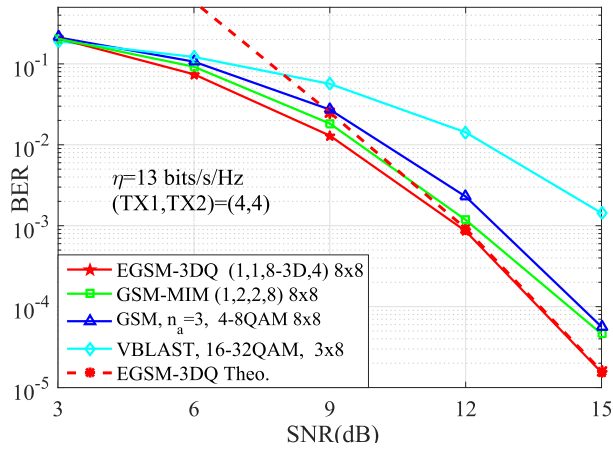


FIGURE 3. BER comparison between simulation and theory for EGSM-3DQ at 13 bits/s/Hz, and compared with GSM-MIM, GSM, and VBLAST.

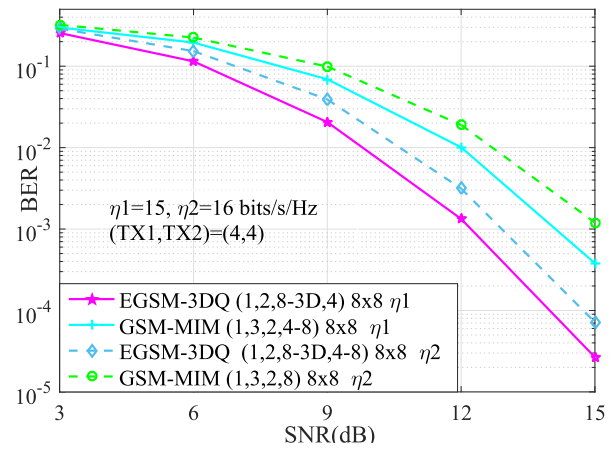


FIGURE 5. BER comparisons of the EGSM-3DQ with the GSM-MIM with  $(TX1, TX2) = (4, 4)$ .

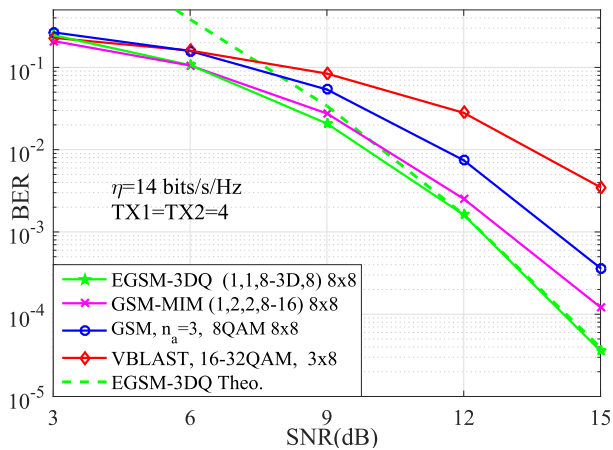


FIGURE 4. BER comparison between simulation and theory for EGSM-3DQ at 14 bits/s/Hz, and compared with GSM-MIM, GSM, and VBLAST.

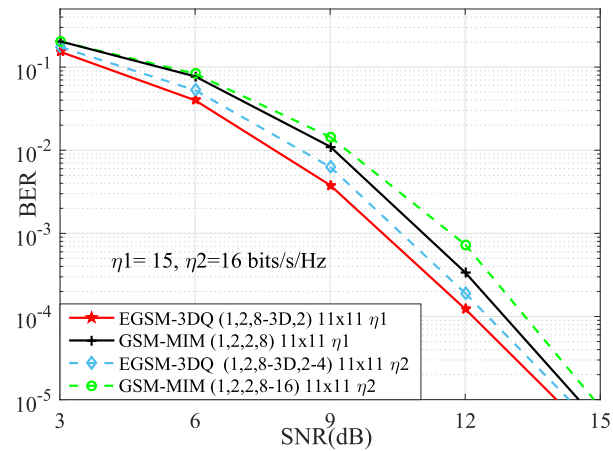


FIGURE 6. BER comparisons of the EGSM-3DQ with the GSM-MIM with  $(TX1, TX2) = (4, 7)$ .

with (1, 3, 2,4-8) and (1, 3, 2, 8), respectively. Due to that the EGSM-3DQ has the bigger squared MED, it will achieve better BER performance. In Fig. 5, the simulation results verify this argument. From the observation of Fig. 5, the

EGSM-3DQ scheme gains around 1.8 dB SNR gain at SE of 15 bits/s/Hz and 2 dB SNR gain at SE of 16 bits/s/Hz over the GSM-MIM scheme at the BER value of  $10^{-3}$ , respectively.

$$\begin{aligned}
 \bar{P}(\mathbf{S} \rightarrow \hat{\mathbf{S}}) &= E_{\mathbf{H}} \left\{ \bar{P}(\mathbf{S} \rightarrow \hat{\mathbf{S}} | \mathbf{H}) \right\} \\
 &= E_{\mathbf{H}} \left\{ Q \left( \sqrt{\frac{1}{2E_{av}\sigma^2}} \cdot \|\mathbf{H} \cdot (\mathbf{S} - \hat{\mathbf{S}})\|^2 \right) \right\} \\
 &= E_{h_{n_r, \mu}} \left\{ \frac{1}{\pi} \int_0^{\frac{\pi}{2}} \exp \left( \frac{-\sum_{\mu=1}^{N_t} \sum_{n_r=1}^{N_r} |h_{n_r, \mu} (\mathbf{S}(\mu) - \hat{\mathbf{S}}(\mu))|^2}{4E_{av}\sigma^2 \sin^2 \theta} \right) d\theta \right\} \\
 &= \frac{1}{\pi} \int_0^{\frac{\pi}{2}} \left( \frac{\sin^2 \theta}{\sin^2 \theta + \frac{\bar{d}_{\mathbf{S}, \min}^2}{4\sigma^2}} \right)^{N_r} d\theta \tag{18}
 \end{aligned}$$

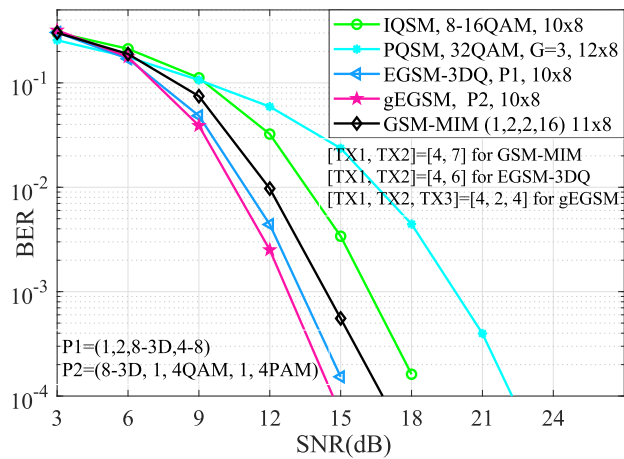


FIGURE 7. BER comparisons of the gEGSM with various systems at 17 bits/s/Hz.

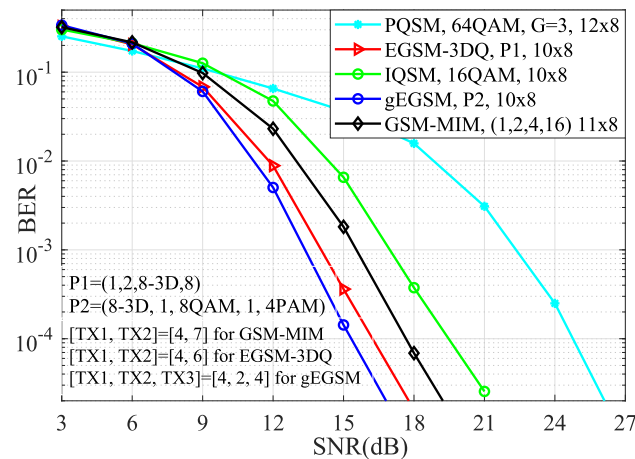


FIGURE 8. BER comparisons of the gEGSM with various systems at 18 bits/s/Hz.

For other number of TAs such as  $N_t = 11$  with the grouping  $(TX1, TX2) = (4, 7)$ , Fig. 6 depicts the BER versus SNR curves of 15, 16 bits/s/Hz for the EGSM-3DQ with (1,2, 8-D,2) and (1,2,8-D,2-4) and the GSM-MIM with (1,2,2,8) and (1,2,2,8-16). It can be observed that about 1 dB SNR gain for 15 bits/s/Hz, 1.2 dB SNR gain for 16 bits/s/Hz are respectively achieved than that of the GSM-MIM system at the BER value of  $10^{-3}$ .

According to the analysis of TABLE 4, the proposed gEGSM has bigger squared MED than other schemes such as EGSM-3DQ, GSM-MIM at the same SEs, it means that the gEGSM will reduce the BER values in comparison with other systems. Fig. 7 and Fig. 8 with the SEs of 17 and 18 bits/s/Hz are depicted and verify the BER performances of the gEGSM, and compared with that of the IQSM, PQSM, GSM-MIM and EGSM-3DQ schemes. For the SE of 17 bits/s/Hz in Fig. 7, due to the bigger squared MED provided in 4, the gEGSM with (8-3D, 1, 4QAM, 1, 4PAM) outperforms the IQSM with 8-16QAM, PQSM with 32QAM, GSM-MIM with (1,2,2,16)

and EGSM-3DQ with (1, 2, 8-3D, 4-8) in terms of BER performance. For instance, approximately 0.6 dB, 2 dB, 3.5 dB, 6.5 dB SNR gain over the EGSM-3DQ, GSM-MIM, IQSM, PQSM are achieved at the BER value of  $10^{-3}$ , respectively. Also, for the SE of 18 bits/s/Hz in Fig. 7 with the change of the modulation order, compared with other schemes, the gEGSM still has better BER performance, which verifies the advantage of the gEGSM scheme.

## VI. CONCLUSION

In this paper, in order to increase the SE and enhance the reliability of communication link, the EGSM-3DQ is proposed to further exploit the index domain by combining active AI combinations with the design of the improved 3D signal constellation. Then, the 3D Signal Mapper and AI vector Modulator is designed in detail for extending the active AI combinations. Furthermore, the gEGSM is proposed to further improve the SE and BER performance. Finally, the comparisons for the squared MEDs between the proposed schemes and GSM-MIM are provided and the average BEP is analyzed. Numerical results show that the proposed schemes outperform other schemes such as GSM, GSM-MIM, IQSM, PQSM at the same transmit rate in terms of BER performance.

## REFERENCES

- [1] R. Y. Mesleh, H. Haas, S. Sinanovic, C. W. Ahn, and S. Yun, "Spatial modulation," *IEEE Trans. Veh. Technol.*, vol. 57, no. 4, pp. 2228–2241, Jul. 2008.
- [2] J. Fu, C. Hou, W. Xiang, L. Yan, and Y. Hou, "Generalised spatial modulation with multiple active transmit antennas," in *Proc. IEEE GLOBECOM Workshops*, Miami, FL, USA, Dec. 2010, pp. 839–844.
- [3] T. Data, H. S. Eshqaraiah, and A. Chockalingam, "Generalized space and frequency index modulation," *IEEE Trans. Veh. Technol.*, vol. 65, no. 6, pp. 4911–4924, Jul. 2016.
- [4] J. Wang, S. Jia, and J. Song, "Generalised spatial modulation system with multiple active transmit antennas and low complexity detection scheme," *IEEE Trans. Wireless Commun.*, vol. 11, no. 4, pp. 1605–1615, Apr. 2012.
- [5] R. Mesleh, S. S. Ikki, and H. M. Aggoune, "Quadrature spatial modulation," *IEEE Trans. Veh. Technol.*, vol. 64, no. 6, pp. 2738–2742, Jun. 2015.
- [6] K. Gunde and A. Sundru, "Modified generalized quadrature spatial modulation performance over Nakagami-m fading channel," *Int. J. Commun. Syst.*, vol. 34, no. 16, p. e4944, 2021.
- [7] J. Li, S. Dang, Y. Yan, Y. Peng, S. Al-Rubaye, and A. Tsourdos, "Generalized quadrature spatial modulation and its application to vehicular networks with NOMA," *IEEE Trans. Intell. Transp. Syst.*, vol. 22, no. 7, pp. 4030–4039, Jul. 2021.
- [8] L. Wang, "Generalized quadrature space-frequency index modulation for MIMO-OFDM systems," *IEEE Trans. Commun.*, vol. 69, no. 9, pp. 6375–6389, Sep. 2021.
- [9] F. Huang, X. Liu, Z. Zhou, J. Luo, and J. Wang, "Quadrature index modulation with three-dimension constellation," *IEEE Access*, vol. 7, pp. 182335–182347, 2019.
- [10] F. Huang and Y. Zhan, "Design of spatial constellation for spatial modulation," *IEEE Wireless Commun. Lett.*, vol. 9, no. 7, pp. 1097–1100, Jul. 2020.
- [11] C.-C. Cheng, H. Sari, S. Sezginer, and Y. T. Su, "Enhanced spatial modulation," *IEEE Trans. Commun.*, vol. 63, no. 6, pp. 2237–2248, Jun. 2015.
- [12] C.-C. Cheng, H. Sari, S. Sezginer, and Y. T. Su, "New signal designs for enhanced spatial modulation," *IEEE Trans. Wireless Commun.*, vol. 15, no. 11, pp. 7766–7777, Nov. 2016.
- [13] Y. Zhan and F. Huang, "Generalized spatial modulation with multi-index modulation," *IEEE Commun. Lett.*, vol. 24, no. 3, pp. 585–588, Mar. 2020.
- [14] B. Vo and H. H. Nguyen, "Improved quadrature spatial modulation," in *Proc. IEEE 86th Veh. Technol. Conf. (VTC-Fall)*, Toronto, ON, Canada, Sep. 2017, p. 24.

- [15] W. Zhao, Z. Huang, F. Huang, and Y. Zhan, "Double generalized spatial modulation," *Trans. Emerg. Telecommun. Technol.*, vol. 33, no. 1, p. e4386, Jan. 2022.
- [16] W. Qu, M. Zhang, X. Cheng, and P. Ju, "Generalized spatial modulation with transmit antenna grouping for massive MIMO," *IEEE Access*, vol. 5, pp. 26798–26807, 2017.
- [17] F. R. Castillo-Soria, J. Cortez-González, R. Ramirez-Gutierrez, F. M. Maciel-Barboza, and L. Soriano-Equigua, "Generalized quadrature spatial modulation scheme using antenna grouping," *ETRI J.*, vol. 39, no. 5, pp. 707–717, Oct. 2017.
- [18] G. Huang, C. Li, S. Aissa, and M. Xia, "Parallel quadrature spatial modulation for massive MIMO systems with ICI avoidance," *IEEE Access*, vol. 7, pp. 154750–154760, 2019.
- [19] M. K. Simon and M. Alouini, *Digital Communication Over Fading Channels* (Wiley Series in Telecommunications and Signal Processing), 2nd ed. Hoboken, NJ, USA: Wiley, 2005.



**FUCHUN HUANG** received the M.E. degree from Jiangsu University, in 2012, and the doctoral degree from Sun Yat-sen University, China, in 2020, all in telecommunication and information systems. His current research interests include index modulation, spatial constellation design, antenna selection algorithms, and OFDM.

• • •



**PING YU** received the B.E. degree in electronics information engineering from Guangxi University, in 2004, and the M.E. degree in computer science and technology from the South China University of Technology, China, in 2010. Her research interests include MIMO, spatial modulation, and the Internet of Things.